PHYSICAL REVIEW B **88**, 205415 (2013)

Quantum transport theory with nonequilibrium coherent potentials

Yu Zhu,[1,*] Lei Liu,[1] and Hong Guo[2,1]
[1]*NanoAcademic Technologies Inc., 7005 Blvd. Taschereau, Brossard, QC, Canada J4Z 1A7*
[2]*Department of Physics, McGill University, Montreal, QC, Canada H3A 2T8*
(Received 9 May 2013; published 13 November 2013)

Since any realistic electronic device has some degree of disorder, predicting disorder effects in quantum transport is a critical problem. Here, we report the theory of nonequilibrium coherent potential approximation (NECPA) for analyzing disorder effects in nonequilibrium quantum transport of nanoelectronic devices. The NECPA is formulated by contour-ordered nonequilibrium Green's function where the disorder average is carried out within the coherent potential approximation on the complex-time contour. We have derived a set of rules that supplement the celebrated Langreth theorem and, as a whole, the generalized Langreth rules allow us to derive NECPA equations for real-time Green's functions. The solution of NECPA equations provides the disorder-averaged nonequilibrium density matrix as well as other relevant quantities for quantum transport calculations. We establish the excellent accuracy of NECPA by comparing its results to brute force numerical calculations of disordered tight-binding models. Moreover, the connection of NECPA equations which are derived on the complex-time contour to the nonequilibrium vertex correction theory which is derived on the real-time axis is made. As an application, we demonstrate that NECPA can be combined with density functional theory to enable analysis of nanoelectronic device physics from atomistic first principles.

DOI: 10.1103/PhysRevB.88.205415 PACS number(s): 85.35.−p, 73.63.−b, 73.23.Ad, 72.80.Ng

I. INTRODUCTION

As dimensional scaling of electronic devices continues, quantum effects of electron conduction is becoming increasingly important for practical design of emerging systems. A theory typically starts from a given device Hamiltonian from which quantum transport is analyzed by techniques such as the scattering matrix and/or Keldysh nonequilibrium Green's function (NEGF) methods.[1,2] Calculation of device Hamiltonian under the realistic condition of device operation is, however, a very complicated problem and most device simulations rely on model and/or parametrized Hamiltonians including the effective mass Hamiltonian, the $\mathbf{k}\cdot\mathbf{p}$ Hamiltonian, the tight-binding Hamiltonian, etc. Combined with the NEGF formalism for quantum transport, these approaches provide important insights for understanding nanoelectronic device physics. However, there is a clear need in the physics community to advance atomistic first principles, parameter-free and self-consistent methods to fundamentally solve emerging nanoelectronic device problems. This is necessary not only due to the lack of reliable phenomenological Hamiltonian parameters for many materials and structures, but also due to the fact that transport driven by an external bias is intrinsically a nonequilibrium problem while parametrization of model Hamiltonian has usually been done at equilibrium. Quantum transport theory at the atomistic level is also necessary because the number of atoms in emerging generations of practical devices is becoming countable.

One of the most basic requirements for any atomistic formalism of nonequilibrium quantum transport is the ability to handle effects of disorder. This is because all realistic device materials contain some degree of unavoidable and random disorder such as atomic defects, vacancies, surface roughness, interface irregularities, etc. In addition, for many situations, the disorder is created by impurity doping in order to functionalize the material such as semiconductors. Because the device Hamiltonian depends on the configuration of the disorder, the predicted physical properties must be averaged over the multitudes of disorder configurations. Disorder average can be carried out by generating many disorder configurations for a given disorder concentration. However, such brute force analysis is computationally prohibitive in atomistic modeling of realistic nanodevices. To overcome the prohibitively large computation required for performing configuration average of disorder, it is desired to obtain the averaged physical quantity without computing each impurity configuration individually. In this regard, a well-developed technique in electronic-structure theory is the coherent potential approximation (CPA).[3] CPA is an effective medium technique by which the disorder average of retarded Green's function $\overline{G^r}$ can be carried out analytically. The CPA method is originally developed to study disordered bulk materials[3] and later extended to investigate disorder effects in surfaces and interfaces.[4]

Recently, significant progresses have been achieved to understand disorder scattering in quantum transport by extending CPA with vertex correction technique.[5] In Ref. 6, Carva *et al*. calculated disorder-averaged conductance in the linear response regime by using vertex correction and the results were in good agreement to those of supercell calculation. In Ref. 7, one of the authors and collaborators advanced the nonequilibrium vertex correction (NVC) theory which applied vertex correction technique to NEGF and obtained disorder-averaged lesser Green's function $\overline{G^<}$ in addition to $\overline{G^r}$. Since important physical quantities in quantum transport can be expressed in terms of $\overline{G^r}$ and $\overline{G^<}$ (see Sec. II), the first-principles CPA-NVC approach has been successfully applied to investigate a variety of nonequilibrium quantum transport problems including disorder effects in magnetic tunnel junctions,[7,8] Cu interconnects,[9] impurity limited mobility of short channel graphene,[10] etc.

While the CPA-NVC theory is practically very useful, there are important unresolved issues that require further theoretical investigation, for instance, (i) two different approximations,

CPA for $\overline{G^r}$ and NVC for $\overline{G^<}$, are used in the CPA-NVC theory. It is, however, not proved that these two approximations are actually consistent with each other at nonequilibrium, although it has been numerically verified as such at equilibrium.[7] (ii) So far, the NVC theory has been limited to situations involving binary disorder sites, namely, a site labeled q can be occupied by two species A or B with their respective statistical weights. There are, however, many important nonequilibrium transport problems that involve multiple species $q = A, B, C, \ldots$. How to extend CPA-NVC theory to multiple species, as can be done in CPA, is nontrivial and has not been achieved. (iii) So far, the NVC equation has been solved either directly or iteratively. The direct solution requires solving an extremely large linear equation array while the iterative solution is not always numerically stable. It is necessary to develop a different method to solve $\overline{G^<}$ efficiently and smoothly, especially for systems with low-disorder concentration.

In this work, we shall develop a completely different approach[11] other than the vertex correction technique. The key idea is based on the fact that the retarded Green's function and the contour-ordered Green's function have the same mathematical structure, as such the CPA equation for $\overline{G^r}$ can be viewed as the contour-ordered CPA equation. By extending the celebrated Langreth theorem,[12] we analytically continue from the complex-time contour to the real-time axis such that the equations of nonequilibrium coherent potential approximation (NECPA) are derived for both $\overline{G^r}$ and $\overline{G^<}$ simultaneously. Although the NECPA equations look very different from CPA-NVC equations, the two equation sets can be proved to be equivalent to each other. This formulation of NECPA is not only elegant from the theoretical point of view, it also resolves all the theoretical and practical issues mentioned in the last paragraph. Finally, we present the combination of NECPA with the density functional theory (DFT) to investigate nanoelectronic device physics from atomistic first principles.

The rest of the paper is organized as follows. Section II gives a brief review of NEGF formalism. Section III presents the theory of NECPA, which is the key work of this paper. Section IV discusses the connection of NECPA to CPA-NVC. Section V provides numerical verifications of NECPA. Section VI addresses the application of NECPA to DFT. Finally, the paper is summarized in Sec. VII. Some mathematical proofs and technical details are organized in several appendixes.

II. NEGF FOR QUANTUM TRANSPORT

To put the NECPA theory into context and for ease of presentations, in this section we briefly review the NEGF formalism for calculating quantum transport in two-probe systems with disorder. The formalism follows that of Ref. 13.

Consider a general two-probe system consisting of a central scattering region plus the left/right semi-infinite electrodes, schematically shown in Fig. 1. There are disorder sites randomly located in the scattering region indicated by the crossed circles. Theoretically, one may mimic disorder effects by assigning the onsite energy to a random discrete variable.[14] It is assumed that on a disorder site i, the onsite energy ε_i

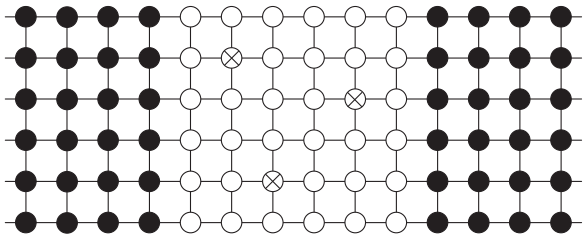

FIG. 1. Schematic plot of a two-probe system with some impurity sites in the central scattering region. The left/right electrodes extend to $z = \pm\infty$. The black dots are sites of electrodes, white circles are pure sites in the scattering region, white sites with a cross are impurity sites.

takes value ε_{iq} with probability x_{iq}, where $q = 1,2,\ldots$ labels multiple impurity species and, clearly, $\sum_q x_{iq} = 1$.

The Hamiltonian of the two-probe system in the second quantization representation can be written as

$$H = H_C + \sum_{\beta=L,R} H_\beta + \sum_{\beta=L,R} H_{C\beta}, \tag{1}$$

$$H_C = \sum_i \varepsilon_i c_i^\dagger c_i + \sum_{i<j} t_{ij} c_i^\dagger c_j + t_{ij}^* c_j^\dagger c_i, \tag{2}$$

$$H_\beta = \sum_k \epsilon_{\beta k} a_{\beta k}^\dagger a_{\beta k}, \tag{3}$$

$$H_{C\beta} = \sum_{ik} t_{ik} c_i^\dagger a_{\beta k} + t_{ik}^* a_{\beta k}^\dagger c_i, \tag{4}$$

where H_C is the Hamiltonian of the central scattering region, H_β ($\beta = L, R$) is the Hamiltonian of the left or right electrode, and $H_{C\beta}$ is the coupling between the scattering region and the β electrode. Note that the above Hamiltonian is in a quadratic form, thus analytical solution of quantum transport can be obtained if the onsite energy ε_i is a definite variable. The complexity of our problem comes from the fact that ε_i is a random variable and hence any physical quantities must be averaged over disorder configurations.

In the NEGF formalism, all physical quantities can be expressed in terms of Green's functions. The most important quantities for a transport theory are the electric current and the occupation number. The current flowing out of the β electrode can be derived as (in atomic units $e = \hbar = 1$)

$$I_\beta = 2\,\mathrm{Re}\int \frac{dE}{2\pi}\mathrm{Tr}\left[\overline{G^r(E)}\Sigma_\beta^<(E) + \overline{G^<(E)}\Sigma_\beta^a(E)\right]. \tag{5}$$

The occupation number of site i is calculated from the lesser Green's function $G^<$:

$$N_i = \mathrm{Im}\int \frac{dE}{2\pi}\mathrm{Tr}[\overline{G^<(E)}]_{ii}, \tag{6}$$

in which $[\ldots]_{ii}$ is to take the diagonal element (diagonal block) of site i. In these expressions, G^r and $G^<$ are the retarded and lesser Green's functions of the central region of the system, and $\Sigma_\beta^<$ and Σ_β^a are the lesser and advanced self-energies of the β electrode. The notation $\overline{(\ldots)}$ means these quantities need to be averaged over disorder configurations $\{\varepsilon_i\}$. The advanced Green's function and the advanced self-energy are Hermitian conjugates of their retarded counterparts

$$G^a(E) = [G^r(E)]^\dagger, \quad \Sigma_\beta^a(E) = [\Sigma_\beta^r(E)]^\dagger.$$

To proceed further, G^r and $G^<$ are solved by the Dyson equation and Keldysh equation, respectively,

$$G^r(E) = \left[E - H_C^0 - \varepsilon - \Sigma^r(E)\right]^{-1}, \tag{7}$$

$$G^<(E) = G^r(E)\,\Sigma^<(E)\,G^a(E), \tag{8}$$

where H_C^0 is the off-diagonal (definite) part of H_C, $\varepsilon \equiv \mathrm{diag}([\varepsilon_1, \varepsilon_2, \ldots])$ is the diagonal (random) part of H_C, and $\Sigma^r(E)$ and $\Sigma^<(E)$ are the retarded and lesser total self-energies

$$\Sigma^r(E) = \Sigma_L^r(E) + \Sigma_R^r(E), \tag{9}$$

$$\Sigma^<(E) = \Sigma_L^<(E) + \Sigma_R^<(E), \tag{10}$$

and

$$\Sigma_\beta^<(E) = f_\beta(E)\left[\Sigma_\beta^a(E) - \Sigma_\beta^r(E)\right]. \tag{11}$$

Here, $f_\beta(E)$ is the Fermi function of the β electrode. Note we have assumed that all disorder sites are located in the central region and electrodes have no disorder. Otherwise, one can always enlarge the central region to include all disorder sites.[15] With this in mind, the disorder average is done to the Green's functions and not to the self-energies of the electrodes.

Another important physical quantity in quantum transport is the transmission coefficient T. Note that the electric current in Eq. (5) can be rewritten as

$$I_L = -I_R = \int \frac{dE}{2\pi} T(E)\left[f_L(E) - f_R(E)\right],$$

in which $T(E)$ is the transmission coefficient which can be expressed in terms of Green's functions,

$$T(E) = \mathrm{Tr}\,\overline{G^r(E)\,\Gamma_L(E)\,G^a(E)\,\Gamma_R(E)}, \tag{12}$$

in which $\Gamma_\beta(E) \equiv -i[\Sigma_\beta^a(E) - \Sigma_\beta^r(E)]$ is the linewidth function of the β electrode. Notice that $\Sigma^<(E)$ is reduced to $\Gamma_L(E)$ by making the substitution $f_L(E) \to -i$ and $f_R(E) \to 0$ in Eqs. (10) and (11). So, the calculation of disorder-averaged transmission $T(E)$ can be reduced to the calculation of $\overline{G^<}$:

$$\begin{aligned} T(E) &= \mathrm{Tr}\,\overline{G^r(E)\,\Gamma_L(E)\,G^a(E)}\Gamma_R(E) \\ &= \mathrm{Tr}\,\overline{G_L^<(E)}\Gamma_R(E), \end{aligned} \tag{13}$$

in which $\overline{G_L^<(E)}$ is defined as

$$\overline{G_L^<(E)} \equiv [\overline{G^<(E)}]_{f_L(E)\to -i,\, f_R(E)\to 0}.$$

With these expressions, all the analysis of disorder effects are reduced to evaluate $\overline{G^r}$ and $\overline{G^<}$ (hereafter, the argument E is omitted for simplicity of notations). In principle, by brute force one can calculate the Green's functions for each disorder configuration and evaluate the average afterward. As mentioned in the Introduction, such a brute force calculation quickly becomes formidable due to the huge number of configurations that scales up exponentially with the number of disorder sites in the two-probe systems. We therefore seek for the approximation technique to evaluate the average analytically.

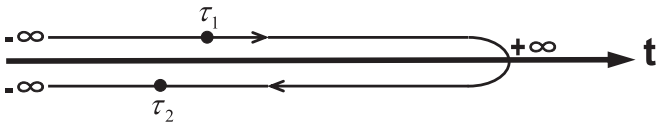

FIG. 2. Schematic plot of the complex-time contour that goes above the real-time axis from $\tau = -\infty$ to $+\infty$, and returns below the real-time axis to $\tau = -\infty$. The contour-ordered Green's function is defined on the complex-time contour. The NECPA equation is derived by analytic continuation of the contour-ordered CPA equation.

III. THEORY OF NECPA

Having discussed the general formalism of NEGF for quantum transport, in this section we present NECPA theory for disordered two-probe systems.

In many-body theory,[16] it is well known that nonequilibrium statistics can be formulated via the contour-ordered Green's function $G(\tau_1, \tau_2)$ where τ_1 and τ_2 are the complex time, as shown in Fig. 2. The key idea of NECPA is to carry out disorder average within CPA to contour-ordered Green's function to obtain $\overline{G(\tau_1, \tau_2)}$. Afterward, we transform the disorder-averaged contour-ordered Green's function $\overline{G}$ to real-time Green's functions $\overline{G^r}$ and $\overline{G^<}$ by analytic continuation.

In the following sections, we first introduce the contour-ordered CPA equation which is the starting point of NECPA theory. We proceed to derive NECPA equations by applying the generalized Langreth theorem to the contour-ordered CPA equation. After that, we discuss the iterative method for solving NECPA equations and the analytical solutions in the low-disorder concentration limit. Finally, we investigate a special but important case, namely, two-probe systems with transverse periodicity.

A. Contour-ordered CPA equation

The spirit of CPA is to replace the random onsite energy $\{\varepsilon_i\}$ in Eq. (7) by an effective onsite energy $\{\tilde{\varepsilon}_i^r\}$ such that the average scattering vanishes with respect to the effective media. Originally, CPA was developed for the retarded Green's function [see, e.g., Eq. (9) of the first paper in Ref. 3]:

$$\begin{aligned} \overline{t_i^r} &= \sum_q x_{iq} t_{iq}^r = 0, \\ t_{iq}^r &\equiv \left[\left(\varepsilon_{iq} - \tilde{\varepsilon}_i^r\right)^{-1} - \overline{G_i^r}\right]^{-1}, \\ \overline{G_i^r} &\equiv [\overline{G^r}]_{ii}, \\ \overline{G^r} &= \left[E - H_C^0 - \tilde{\varepsilon}^r - \Sigma^r\right]^{-1}, \end{aligned} \tag{14}$$

where $\tilde{\varepsilon}^r \equiv \mathrm{diag}([\tilde{\varepsilon}_1^r, \tilde{\varepsilon}_2^r, \ldots])$ is a diagonal matrix of the effective onsite energies which is called the coherent potential in the literature.[3] The first line in Eq. (14) states the sprit of CPA, namely, on the disorder site i, scattering processes due to various impurity species cancel with each other.

Now, we extend the idea of CPA to the contour-ordered Green's function. Since the contour-ordered Green's function and retarded Green's function satisfy the same equation of motion and hence have the same mathematical structure,[1,16] it is straightforward to write the contour-ordered CPA equation

by simply removing the superscript r in Eq. (14), we have

$$\begin{aligned}\overline{t_i} &= \sum_q x_{iq} t_{iq} = 0,\\ t_{iq} &\equiv [(\varepsilon_{iq} - \tilde{\varepsilon}_i)^{-1} - \overline{G_i}]^{-1},\\ \overline{G_i} &\equiv [\overline{G}]_{ii},\\ \overline{G} &= \left[E - H_C^0 - \tilde{\varepsilon} - \Sigma\right]^{-1},\end{aligned} \tag{15}$$

where $\overline{t_i}$, t_{iq}, $\tilde{\varepsilon}_i$, $\overline{G_i}$, $\overline{G}$, Σ are defined on the complex-time contour and have been Fourier transformed to frequency space.

It is more intuitive to rewrite Eq. (15) into an equivalent form by using the conditional Green's function

$$\begin{aligned}\overline{G_i} &= \sum_q x_{iq} \overline{G_{iq}},\\ \overline{G_i} &= \left[\left(E - H_C^0 - \tilde{\varepsilon} - \Sigma\right)^{-1}\right]_{ii},\\ \overline{G_{iq}} &= \left[\left(E - H_C^0 - \tilde{\varepsilon}^{iq} - \Sigma\right)^{-1}\right]_{ii},\end{aligned} \tag{16}$$

where $\tilde{\varepsilon}^{iq}$ means to replace the ith diagonal element of $\tilde{\varepsilon}$ by ε_{iq}. $\overline{G_{iq}}$ is the conditional Green's function, namely, the Green's function of site i under the condition that the site is occupied by species q and other sites remain disorder sites. The first line in Eq. (16) is consistent with the meaning of conditional Green's function. The derivation of the first line in Eq. (16) can be found in Appendix A.

Finally, Eq. (16) can be further reduced to another convenient but equivalence form

$$\begin{aligned}\overline{G_i} &= \sum_q x_{iq} \overline{G_{iq}},\\ \overline{G} &= \left[E - H_C^0 - \tilde{\varepsilon} - \Sigma\right]^{-1},\\ \overline{G_i} &= [\overline{G}]_{ii},\\ \overline{G_i} &= [E - \tilde{\varepsilon}_i - \Omega_i]^{-1},\\ \overline{G_{iq}} &= [E - \varepsilon_{iq} - \Omega_i]^{-1},\end{aligned} \tag{17}$$

where Ω_i is the contour-ordered coherent interactor.[17] Equation (17) will be used in the analytic continuation in the next section. The derivation of the fourth and fifth lines in Eq. (17) can be found in Appendix A.

B. Generalized Langreth theorem and NECPA equations

In this section, we shall apply analytic continuation to the contour-ordered CPA equation (17) to obtain disorder-averaged real-time Green's function. In this regard, one usually applies the Langreth theorem[1,12] that bridges between the contour-ordered Green's function G and the real-time Green's functions $G^{r,a}$ and $G^{<,>}$. According to the Langreth theorem, if contour-ordered quantities A, B, C satisfy $C = AB$, then the corresponding retarded and lesser quantities are obtained as

$$C^r = A^r B^r, \tag{18}$$

$$C^< = A^r B^< + A^< B^a. \tag{19}$$

In addition, if a contour-ordered quantity D does not have a finite imaginary part so that D^r and D^a are indistinguishable, it behaves as a constant

$$D^r = D^a = D, \tag{20}$$

$$D^< = 0. \tag{21}$$

Looking at the form of the contour-ordered CPA equation (17), it is obvious that the above Langreth rules [Eqs. (18)–(21)] can not be directly applied because the right-hand side of the second, fourth, and fifth lines in Eq. (17) involve the inverse operations. Therefore, a different set of Langreth rules need to established to determine quantities like $(A^{-1})^{r,a,<,>}$. This can be accomplished as follows. Let $C = AA^{-1} = 1$ and apply Eqs.(18)–(21), and two rules for the inverse are derived as follows:

$$(A^{-1})^r = (A^r)^{-1}, \tag{22}$$

$$(A^{-1})^< = -(A^r)^{-1} A^< (A^a)^{-1}. \tag{23}$$

These rules allow one to carry out analytic continuation of the inverse of contour-ordered quantities. The two Langreth rules (22) and (23), together with the original rules (18)–(21), shall be referred to as generalized Langreth theorem in the rest of this paper.

By applying the generalized Langreth theorem to the contour-ordered CPA equation (17), two sets of equations can be obtained for $\overline{G^r}$ and $\overline{G^<}$, respectively:

$$\begin{aligned}\overline{G_i^r} &= \sum_q x_{iq} \overline{G_{iq}^r},\\ \overline{G^r} &= \left[E - H_C^0 - \tilde{\varepsilon}^r - \Sigma^r\right]^{-1},\\ \overline{G_i^r} &= [\overline{G^r}]_{ii},\\ \overline{G_i^r} &= \left[E - \tilde{\varepsilon}_i^r - \Omega_i^r\right]^{-1},\\ \overline{G_{iq}^r} &= \left[E - \varepsilon_{iq} - \Omega_i^r\right]^{-1},\end{aligned} \tag{24}$$

$$\begin{aligned}\overline{G_i^<} &= \sum_q x_{iq} \overline{G_{iq}^<},\\ \overline{G^<} &= \overline{G^r}(\Sigma^< + \tilde{\varepsilon}^<)\overline{G^a},\\ \overline{G_i^<} &= [\overline{G^<}]_{ii},\\ \overline{G_i^<} &= \overline{G_i^r}(\tilde{\varepsilon}_i^< + \Omega_i^<)\overline{G_i^a},\\ \overline{G_{iq}^<} &= \overline{G_{iq}^r}\Omega_i^< \overline{G_{iq}^a}.\end{aligned} \tag{25}$$

These two equations are the central results of this work which extends the equilibrium CPA for bulk systems to the nonequilibrium two-probe systems. As expected, the equation of $\overline{G^r}$ recovers the known CPA equation, and $\overline{G^<}$ will be shown to be equivalent to the NVC equation in Ref. 7. This way, by applying the generalized Langreth theorem to the contour-ordered CPA equation, both $\overline{G^r}$ and $\overline{G^<}$ are derived simultaneously. Collectively, in the rest of this paper, we shall refer to Eqs. (24) and (25) as the NECPA equations.

The NECPA theory presented above has several distinct advances at both the fundamental level and the practical level: (i) NECPA treats disorder average for $\overline{G^r}$ and $\overline{G^<}$ on equal footing and the derived equations are similar in form. (ii) NECPA derives the averaged conditional Green's functions $\overline{G_{iq}^r}$ and

$\overline{G^<_{iq}}$ for disorder site with any number of impurity species. (iii) NECPA provides a natural iterative method for solving $\overline{G^r}$ and $\overline{G^<}$, which will be the subject of the next section.

C. Solving the NECPA equations

NECPA equations not only make a theoretical advance, but also provide a natural iterative method for solving $\overline{G^r}$ and $\overline{G^<}$. With the aid of Eq. (24), $\overline{G^r}$ can be solved with following iterative method:

(1) Make an initial guess of Ω^r.

(2) Determine $\tilde{\varepsilon}^r$ from the first, the fourth, and the fifth lines of Eq. (24); the result is

$$\tilde{\varepsilon}^r_i = E - \Omega^r_i - \left[\sum_q x_{iq}\left(E - \varepsilon_{iq} - \Omega^r_i\right)^{-1}\right]^{-1}.$$

(3) Determine $\overline{G^r}$ from the second line of Eq. (24):

$$\overline{G^r} = \left[E - H^0_C - \tilde{\varepsilon}^r - \Sigma^r\right]^{-1}.$$

(4) Update Ω^r by solving it from the fourth line of Eq. (24); the result is

$$\Omega^r_i = E - \tilde{\varepsilon}^r_i - [\overline{G^r}]^{-1}_{ii}.$$

(5) Go back to step 2 to repeat the process until Ω^r is fully converged.

With the aid of Eq. (25), $\overline{G^<}$ can be solved with following iterative method:

(1) Make an initial guess of $\Omega^<$.

(2) Determine $\tilde{\varepsilon}^<$ from the first, the fourth, and the fifth lines of Eq. (25); the result is

$$\tilde{\varepsilon}^<_i = \left(\overline{G^r_i}\right)^{-1}\left[\sum_q x_{iq}\overline{G^r_{iq}}\Omega^<_i\overline{G^a_{iq}}\right]\left(\overline{G^a_i}\right)^{-1} - \Omega^<_i.$$

(3) Determine $\overline{G^<}$ from the second line of Eq. (25):

$$\overline{G^<} = \overline{G^r}(\Sigma^< + \tilde{\varepsilon}^<)\overline{G^a}.$$

(4) Update $\Omega^<$ by solving it from the fourth line of Eq. (25); the result is

$$\Omega^<_i = \left(\overline{G^r_i}\right)^{-1}[\overline{G^<}]_{ii}\left(\overline{G^a_i}\right)^{-1} - \tilde{\varepsilon}^<_i.$$

(5) Go back to step 2 to repeat the process until $\Omega^<$ is fully converged.

Note that quantities $\overline{G^r}$, $\overline{G^a}$, $\overline{G^r_{iq}}$, and $\overline{G^a_{iq}}$ are assumed to be known in the iterative solution to $\overline{G^<}$. In practice, the iterations of $\overline{G^r}$ and $\overline{G^<}$ are actually carried out together.

It is interesting to analyze the computational cost of the above methods. Assume that there are N_D disorder sites in the central region of a two-probe system (see Fig. 1). The costs of steps 2 and 4 are proportional to N_D, while the cost of step 3 is proportional to N^3_D if full matrix operations are used. So, the *bottleneck* of the iteration is step 3 which needs to be carefully optimized. Notice that in two-probe systems, the size along the transport dimension is usually much larger than its transverse dimensions. Taking advantage of this geometry, the cost of step 3 can be drastically reduced using the principal layer approach discussed in the Appendix B.

The computational cost for solving the NECPA equations can be further reduced if the disorder concentration is very low. In typical semiconductor devices, a doping concentration of 10^{20} cm^{-3} (heavily doped) amounts to a disorder concentration $x \sim 2 \times 10^{-3}$. For such low-disorder concentration x, the solution to NECPA equations can be approximated to high precision by analytical expressions obtained by perturbation expansion with respect to the small parameter x. Let $q = 0$ label the host material species and $q > 0$ label impurity species. Low-disorder concentration means $x_{i,q=0} \gg x_{i,q>0}$. We also have $\sum_q x_{iq} = 1$ due to normalization. The solution of NECPA equations can be obtained up to the first order of $x_{i,q>0}$:

$$\tilde{\varepsilon}^r_i \approx \varepsilon_{i0} + \sum_{q>0} x_{iq} t^r_{iq}, \tag{26}$$

$$\tilde{\varepsilon}^<_i \approx \sum_{q>0} x_{iq} t^r_{iq} G^<_{0,ii} t^a_{iq}, \tag{27}$$

in which

$$t^r_{iq} = \left[(\varepsilon_{iq} - \varepsilon_{i0})^{-1} - G^r_{0,ii}\right]^{-1}, \tag{28}$$

$$G^r_0 = \left[E - H^0_C - \varepsilon^0 - \Sigma^r\right]^{-1}, \tag{29}$$

$$G^<_0 = G^r_0 \Sigma^< G^a_0, \tag{30}$$

where $\varepsilon^0 = \mathrm{diag}\left([\varepsilon_{10}, \varepsilon_{20}, \ldots]\right)$ is the onsite energy of host material. These analytical expressions allow one to calculate $\overline{G^r}$ and $\overline{G^<}$ without the iteration procedure discussed above. Using the first order (in x) formula, we found that the total computational cost of transport is roughly twice that of the corresponding clean system.

D. NECPA with transverse periodicity

In some applications, one can identify a small unit cell in the transverse dimensions of two-probe systems. For two-probe systems without disorder, the transverse periodicity allows one to apply the Bloch theorem and make k sampling in the Brillouin zone. Thus, the calculation of the transverse periodic two-probe system is reduced to the calculation in a small unit cell plus k sampling. For two-probe systems with random disorder, the translational symmetry is broken in the transverse dimensions and Bloch theorem does not hold. Nevertheless, NECPA is an effective medium theory whose application restores the translational symmetry of $\overline{G^r}$ and $\overline{G^<}$. Therefore, one can still work with the small unit cell plus k sampling to calculate $\overline{G^r}$ and $\overline{G^<}$.

For transverse periodic two-probe systems, NECPA equations need to be modified slightly to include k sampling:

$$\begin{aligned}
\overline{G^r_i} &= \sum_q x_{iq}\overline{G^r_{iq}},\\
\overline{G^r}(k) &= \left[E - H^0_C(k) - \tilde{\varepsilon}^r - \Sigma^r(k)\right]^{-1},\\
\overline{G^r} &= \int_{-\pi}^{+\pi}\frac{dk}{2\pi}\overline{G^r}(k),\\
\overline{G^r_i} &= [\overline{G^r}]_{ii},\\
\overline{G^r_i} &= \left[E - \tilde{\varepsilon}^r_i - \Omega^r_i\right]^{-1},\\
\overline{G^r_{iq}} &= \left[E - \varepsilon_{iq} - \Omega^r_i\right]^{-1}.
\end{aligned} \tag{31}$$

$$\begin{aligned}
\overline{G_i^<} &= \sum_q x_{iq}\overline{G_{iq}^<},\\
\overline{G^<}(k) &= \overline{G^r}(k)[\Sigma^<(k)+\tilde{\varepsilon}^<]\overline{G^a}(k),\\
\overline{G^<} &= \int_{-\pi}^{+\pi}\frac{dk}{2\pi}\overline{G^<}(k),\\
\overline{G_i^<} &= [\overline{G^<}]_{ii},\\
\overline{G_i^<} &= \overline{G_i^r}(\tilde{\varepsilon}_i^< + \Omega_i^<)\overline{G_i^a},\\
\overline{G_{iq}^<} &= \overline{G_{iq}^r}\Omega_i^<\overline{G_{iq}^a}.
\end{aligned} \tag{32}$$

In the above equations, $H_C^0(k)$ and $\Sigma^{r,<}(k)$ are the Fourier transform of H_C^0 and $\Sigma^{r,<}$. k is the dimensionless wave vector: For systems with periodicity in one transverse dimension, k is defined as $\mathbf{k}\cdot\mathbf{a}$ in which $\mathbf{k}$ is the wave vector and $\mathbf{a}$ is the unit cell vector of the periodic transverse dimension. For systems with periodicity in two transverse dimensions, k is defined as $(k_1,k_2)=(\mathbf{k}\cdot\mathbf{a}_1,\mathbf{k}\cdot\mathbf{a}_2)$ in which $\mathbf{a}_1$ and $\mathbf{a}_2$ are the two unit-cell vectors of the periodic transverse dimensions. Correspondingly, $\int_{-\pi}^{+\pi}\frac{dk}{2\pi}$ should be understood as $\int_{-\pi}^{+\pi}\frac{dk_1}{2\pi}\int_{-\pi}^{+\pi}\frac{dk_2}{2\pi}$.

IV. FURTHER DISCUSSIONS

This section is devoted to establish the connection of the NECPA theory to the existing CPA-NVC theory.[7] Three issues are discussed in the following sections: the equivalence of NECPA theory and CPA-NVC theory, a disorder-averaged Ward-type identity, and conditional Green's function in binary systems.

A. Equivalence of NECPA and CPA-NVC

In CPA-NVC theory, $\overline{G^<}$ is calculated by using the NVC technique where $\overline{G^<}$ is decomposed into two parts, a simple averaged term and a vertex correlation term, namely,

$$\begin{aligned}
\overline{G^<} &= \overline{G^r\Sigma^<G^a},\\
&= \overline{G^r}\Sigma^<\overline{G^a} + \overline{G^r}\Lambda\overline{G^a},
\end{aligned} \tag{33}$$

in which Λ is a diagonal matrix diag$([\Lambda_1,\Lambda_2,\ldots])$ and is referred to as nonequilibrium vertex correction. Λ satisfies the following NVC equation:[7]

$$\begin{aligned}
\Lambda_i &= \sum_q x_{iq}t_{iq}^r[\overline{G^r}(\Sigma^<+\Lambda)\overline{G^a}]_{ii}t_{iq}^a\\
&\quad - \sum_q x_{iq}t_{iq}^r\overline{G_i^r}\Lambda_i\overline{G_i^a}t_{iq}^a,
\end{aligned} \tag{34}$$

in which $t_{iq}^r \equiv [(\varepsilon_{iq}-\tilde{\varepsilon}_i^r)^{-1}-\overline{G_i^r}]^{-1}$. It is not obvious at all that $\overline{G^<}$ solved from Eqs. (33) and (34) are the same as the solution of Eq. (25) in the NECPA theory.

The differences between NECPA theory and CPA-NVC theory come from distinct theoretical paths. In the CPA-NVC theory, one starts from contour ordered G and derives the Dyson equation (7) for G^r and the Keldysh equation (8) for $G^<$ by analytic continuation. Afterward, disorder average is carried out with CPA and NVC techniques to obtain $\overline{G^r}$ and $\overline{G^<}$. In the NECPA theory, one also starts from the contour ordered G, but the disorder average is carried out by CPA to obtain $\overline{G}$ before the analytic continuation. Afterward, $\overline{G^r}$ and $\overline{G^<}$ are derived on equal footing by applying analytic continuation to $\overline{G}$. Therefore, $\overline{G^<}$ derived by the two theories must be equivalent although the mathematical forms look very different. Explicitly, we are able to prove the equivalence by showing that the nonequilibrium vertex correction Λ in CPA-NVC theory is actually identical to the lesser coherent potential $\tilde{\varepsilon}^<$ in NECPA theory. The proof is presented in Appendix C.

B. Disorder-averaged Ward-type identity

In the NEGF formalism, there is a Ward-type identity which links $G^{r,a}$ to $G^{<,>}$:

$$G^r - G^a \equiv G^> - G^<. \tag{35}$$

By disorder averaging on both sides, one obtains

$$\overline{G^r} - \overline{G^a} \equiv \overline{G^>} - \overline{G^<}. \tag{36}$$

If the disorder average is done *rigorously*, this disorder-averaged identity is obviously true. However, in CPA-NVC theory, approximation techniques are used to carry out disorder average: CPA is applied to the left-hand side of Eq. (36) while NVC to the right-hand side. It was shown by numerical computation at equilibrium[7] that Eq. (36) holds true to extremely high precision for many disordered structures. It is indeed amazing that the equality holds even after making approximations on the two sides.[18]

From the point of view of NECPA, the identity (36) is, however, self-evident: coherent potential approximation is made to the contour-ordered Green's function and afterward all real-time Green's functions $\overline{G^{r,a}}$ and $\overline{G^{<,>}}$ are derived from analytic continuation without further approximation. That is why the identity still holds even after disorder average. In Appendix C, we have proved the equivalence of NECPA theory and CPA-NVC theory which indirectly proves that CPA and NVC are consistent approximations. Finally, we would like to mention that the disorder-averaged identity is very useful to test codes in the numerical implementation.

C. Conditional Green's functions for binary systems

For systems having binary disorder sites, i.e., $q=A,B$, there is an alternative method, the random variable method, to partition $\overline{G_i^r}$ and $\overline{G_i^<}$ into conditional Green's functions $\overline{G_{iq}^r}$ and $\overline{G_{iq}^<}$. Define random variables η_{iA} and η_{iB}: $\eta_{iq}=1$ if site i is occupied by species q and $\eta_{iq}=0$ otherwise. It follows that $\overline{\eta_{iA}}=x_{iA}$, $\overline{\eta_{iB}}=x_{iB}$, and

$$\begin{aligned}
\eta_{iA}+\eta_{iB} &= 1,\\
\eta_{iA}\varepsilon_{iA}+\eta_{iB}\varepsilon_{iB} &= \varepsilon_i.
\end{aligned}$$

By definition, $\overline{G_{iq}^r}$ and $\overline{G_{iq}^<}$ can be expressed in terms of η_{iq}:

$$\overline{G_{iq}^r} = \frac{\overline{\eta_{iq}G_i^r}}{\overline{\eta_{iq}}}, \quad \overline{G_{iq}^<} = \frac{\overline{\eta_{iq}G_i^<}}{\overline{\eta_{iq}}},$$

where $G_i^r=[G^r]_{ii}$ and $G_i^<=[G^<]_{ii}$.

After some algebra,[19] $\overline{G_{iq}^r}$ and $\overline{G_{iq}^<}$ can be derived as

$$\begin{aligned}
\overline{G_{iA}^r} &= \frac{1}{x_{iA}}(\varepsilon_{iA}-\varepsilon_{iB})^{-1}\left(\tilde{\varepsilon}_i^r-\varepsilon_{iB}\right)\overline{G_i^r},\\
\overline{G_{iB}^r} &= \frac{1}{x_{iB}}(\varepsilon_{iB}-\varepsilon_{iA})^{-1}\left(\tilde{\varepsilon}_i^r-\varepsilon_{iA}\right)\overline{G_i^r},
\end{aligned} \tag{37}$$

$$\overline{G_{iA}^<} = \frac{1}{x_{iA}}(\varepsilon_{iA}-\varepsilon_{iB})^{-1}\left[\left(\tilde{\varepsilon}_i^r-\varepsilon_{iB}\right)\overline{G_i^<}+\tilde{\varepsilon}_i^<\overline{G_i^a}\right],$$
$$\overline{G_{iB}^<} = \frac{1}{x_{iB}}(\varepsilon_{iB}-\varepsilon_{iA})^{-1}\left[\left(\tilde{\varepsilon}_i^r-\varepsilon_{iA}\right)\overline{G_i^<}+\tilde{\varepsilon}_i^<\overline{G_i^a}\right]. \quad (38)$$

It can be easily verified that $x_{iA}\overline{G_{iA}^r}+x_{iB}\overline{G_{iB}^r}=\overline{G_i^r}$ and $x_{iA}\overline{G_{iA}^<}+x_{iB}\overline{G_{iB}^<}=\overline{G_i^<}$ as required by the physical meaning of conditional Green's functions. In CPA-NVC theory, conditional Green's functions were calculated with these expressions.[7]

It is shown in Appendix D that by solving $\overline{G_{iq}^r}$ and $\overline{G_{iq}^<}$ from NECPA, Eqs. (24) and (25) for binary disorder site $q=A,B$, the results are identical to Eqs. (37) and (38). For disorder site with more than two impurity species, Eqs. (37) and (38) do not apply, and one has to rely on NECPA equations to calculate conditional Green's functions.

V. NUMERICAL VERIFICATION OF NECPA

Having established the NECPA theoretical framework, in this section we use simple tight-binding (TB) models in one- and two dimensions (1D, 2D) to demonstrate the numerical accuracy of this theory.

A. One-dimensional two-probe system

In this section, NECPA theory is applied to study a 1D TB model which extends from $z=-\infty$ to $+\infty$ and contains two scatterers in the central region, as shown in the inset of Fig. 3(a). The black dots represent clean sites having o-site energy ε_0; the gray dots represent the disorder sites having onsite energy ε_i which is a discrete random variable taking values ε_{iq} $(q=1,2,\ldots)$ with probability x_{iq}. Only nearest neighbors have interactions with a coupling strength t. Due to the simplicity of the 1D TB model, the disorder average can be done *exactly* by brute force enumeration of all possible disorder configurations. For comparison, we shall calculate the transmission coefficient $T(E)$ both by NECPA equations and by brute force enumeration.

For the NECPA calculation, disorder-averaged Green's functions are calculated by using Eqs. (24) and (25). For the 1D TB model, the NECPA equations are drastically simplified and the formula is listed in Appendix E. For brute force enumeration, disorder-averaged Green's function are calculated directly from its definition, namely,

$$\overline{G^r} = \sum_{q_1}\sum_{q_2} x_{1q_1}x_{2q_2}G^r_{q_1q_2},$$
$$G^r_{q_1q_2} = \left[E-\begin{pmatrix}\varepsilon_{1q_1} & t\\ t & \varepsilon_{2q_2}\end{pmatrix}-\begin{pmatrix}\Sigma_0^r & 0\\ 0 & \Sigma_0^r\end{pmatrix}\right]^{-1},$$
$$\overline{G^<} = \sum_{q_1}\sum_{q_2} x_{1q_1}x_{2q_2}G^<_{q_1q_2},$$
$$G^<_{q_1q_2} = G^r_{q_1q_2}\begin{pmatrix}if_L\Gamma_0 & 0\\ 0 & if_R\Gamma_0\end{pmatrix}G^a_{q_1q_2},$$

in which $f_{L,R}$ are Fermi functions of the left and right electrodes, $\Gamma_0=-2\,\mathrm{Im}\Sigma_0^r$ is the linewidth function of the electrode. Σ_0^r is the retarded self-energy of the electrode which can be evaluated analytically for the semi-infinite 1D chain

$$\Sigma_0^r = \xi\left(\frac{E+i0^+-\varepsilon_0}{t}\right)t,$$

where

$$\xi(z)=\frac{z-i\sqrt{4-z^2}}{2},$$

in which the branch of the square root is chosen as $\mathrm{Re}\sqrt{z}>0$.

Transmission coefficient $T(E)$ can be calculated with the aid of disorder-averaged Green's functions. Figure 3 plots $T(E)$ at various disorder concentrations x calculated by three methods: the brute force enumeration; NECPA by evaluating Eqs. (E1) and (E2) in Appendix E; and a CPA′ method which is identical to NECPA but neglecting contributions of the lesser coherent potential $\tilde{\varepsilon}^<$. In Fig. 3(a), $T(E)$ is plotted in the clean limit $x=0$ which is an integer steplike curve coinciding with the number of conducting channels. In Figs. 3(b)–3(f), $T(E)$ is plotted with the increase of x. For clarity and to show the effects of disorder scattering, a background transmission at $x=0$, $T_0\equiv[T(E)]_{x=0}$, has been subtracted from $[T(E)]_{x>0}$. Several observations are in order: (i) Transmission is suppressed gradually with the increase of x which is a clear effect due to disorder scattering. The suppression of $T(E)$ by disorder is more pronounced in the vicinity of the band edge. (ii) Results from NECPA agree quite well with the exact results in full ranges of the disorder concentration, providing a verification of the NECPA formalism. (iii) The CPA′ solution has a noticeable deviation from the exact results, indicating the importance of the lesser coherent potential.

B. Two-dimensional two-probe model

In this section, NECPA theory is applied to study a 2D TB model which is periodic in the transverse direction and contains a single layer of scatterers in the central region, as shown in the inset of Fig. 4(a). As in the 1D TB model, the black dots represent clean sites having onsite energy ε_0; the gray dots represent the disorder sites having onsite energy ε_i which is a discrete random variable taking values ε_{iq} $(q=1,2,\ldots)$ with probability x_{iq}. Only nearest neighbors have interactions with a coupling strength t. For the 2D TB model, exact enumeration becomes impossible since the layer of scatterers contains infinite number of disorder sites. Alternatively, the disorder average can be done by Monte Carlo simulation in a supercell. For comparison, we shall calculate the transmission coefficient $T(E)$ both by NECPA equations and by brute force supercell simulation.

For NECPA calculation, disorder-averaged Green's functions are calculated by using Eqs. (31) and (32). The 2D TB model illustrates how NECPA equations are applied to two-probe systems with periodicity in the transverse direction and the formula is listed in Appendix E. For brute force supercell simulation, we construct a supercell of the two-probe system [see inset of Fig. 4(a)] and disorder sites inside the supercell are occupied randomly according to the probability x_{iq}. As long as the supercell is sufficiently large in the transverse direction, the physics of a supercell two-probe system mimics that of an infinite periodic two-probe system. In our simulation, the supercell contains 1000 rows and

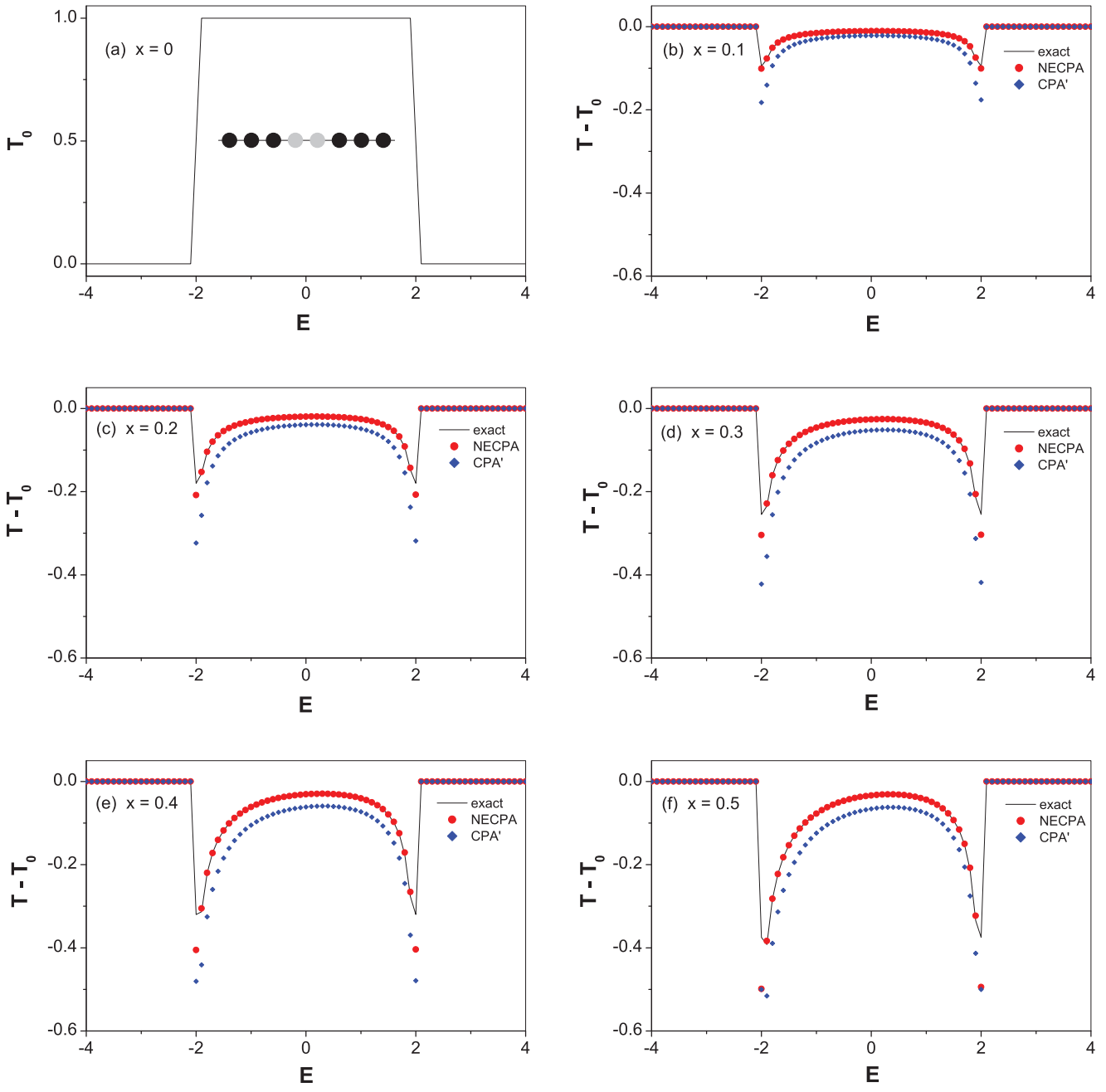

FIG. 3. (Color online) Transmission coefficient T versus energy E at various disorder concentrations x for 1D two-probe system. Three methods are used for comparison: the exact solution, the NECPA method, and the CPA′ method that neglects the lesser coherent potential $\tilde{\varepsilon}^<$ from the NECPA method. Each subfigure is for a different disorder concentration x. The inset of (a) shows the 1D TB model. Other parameters are $\varepsilon_0 = 0$, $t = 1$, $\varepsilon_{1A} = \varepsilon_{2A} = 0$, $x_{1A} = x_{2A} = 1 - x$, $\varepsilon_{1B} = \varepsilon_{2B} = 0.5$, $x_{1B} = x_{2B} = x$.

transmission is averaged over 100 randomly generated disorder configurations.

Transmission coefficient $T(E)$ can be calculated with the aid of disorder-averaged Green's functions. Figure 4 plots $T(E)$ at various disorder concentrations x calculated by three methods: the brute force supercell simulation as described above; NECPA by evaluating Eqs. (E3) and (E4) in Appendix E; and a CPA′ method which is identical to NECPA but neglecting contributions of the lesser coherent potential $\tilde{\varepsilon}^<$. In Fig. 4(a), $T(E)$ is plotted in the clean limit $x = 0$ which can be well understood by the 2D band structure of the TB model (not shown). In Figs. 4(b) to 4(f), $T(E)$ is plotted with the increase of x. For clarity and to show effects of disorder scattering, a background transmission at $x = 0$, $T_0 \equiv [T(E)]_{x=0}$, has been subtracted from $[T(E)]_{x>0}$. Several observations are in order: (i) Transmission is suppressed gradually with the increase of x due to disorder scattering and the suppression is more pronounced near the energies where $T(E)$ changes rapidly. (ii) Results from NECPA agree quite well with the supercell results in full ranges of the disorder concentration, providing a verification of the NECPA formalism. (iii) The CPA′ solution has a noticeable deviation from the

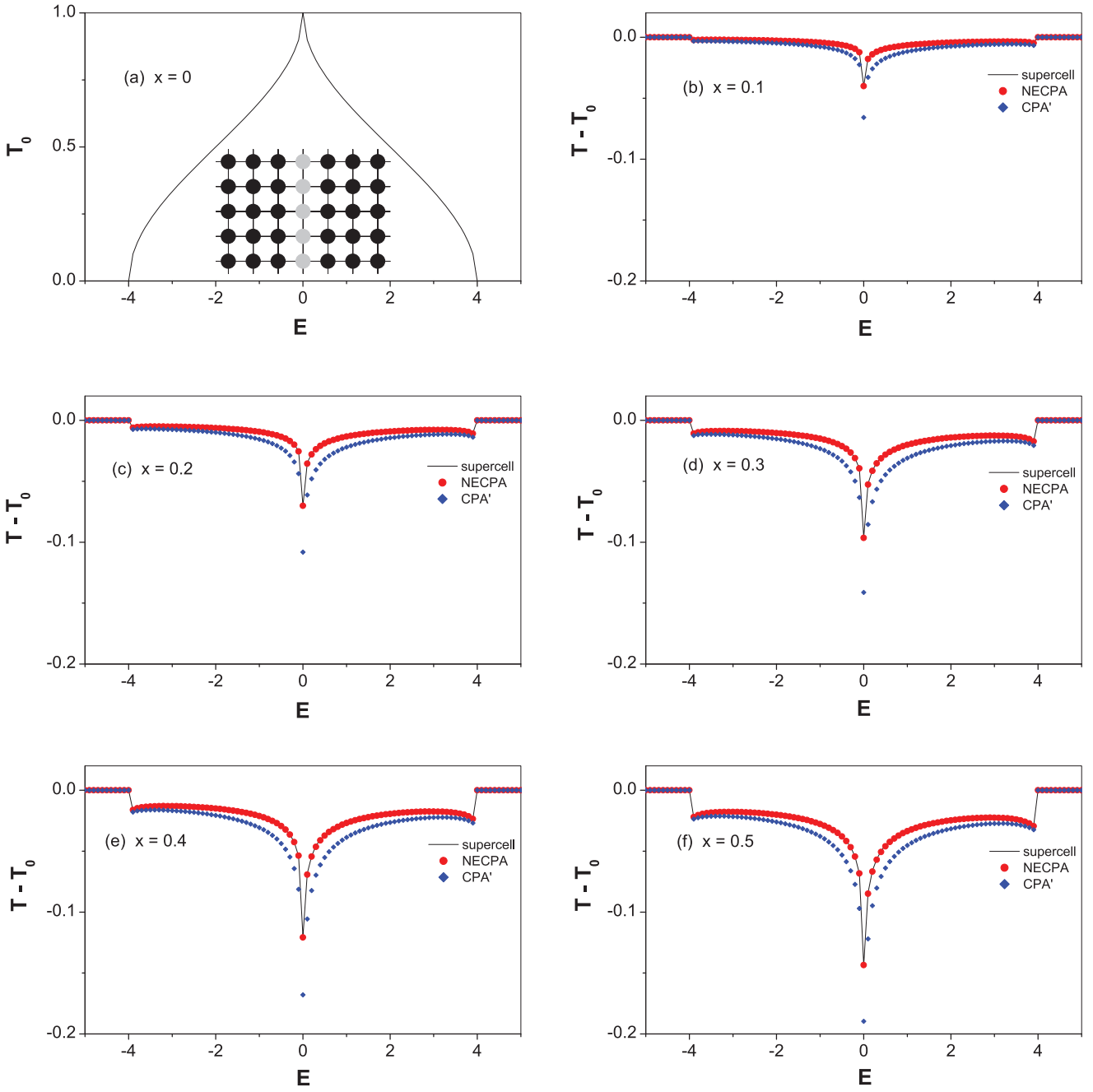

FIG. 4. (Color online) Transmission coefficient T versus energy E at various disorder concentrations x for the 2D two-probe system. Three methods are used for comparison: the supercell solution, the NECPA method, and the CPA′ method that neglects the lesser coherent potential $\tilde{\varepsilon}^<$ from the NECPA method. Each subfigure is for a different disorder concentration x. The inset of (a) shows the 2D TB model which is periodic in the transverse direction. Other parameters are $\varepsilon_0 = 0$, $t = 1$, $\varepsilon_A = 0$, $x_A = 1 - x$, $\varepsilon_B = 0.5$, $x_B = x$.

exact results, indicating the importance of the lesser coherent potential.

VI. APPLICATION OF NECPA TO DFT

As discussed in the Introduction, all realistic device materials contain some degree of random disorders including atomic defects, vacancies, surface roughness, interface irregularities, and dopants, etc. The NECPA formalism presented above provides exciting opportunities to investigate disorder effects in nanoelectronic systems from atomistic first principles. Without disorders, the NEGF-DFT first-principles formalism has been widely applied to analyze nonlinear and nonequilibrium quantum transport properties of nanoelectronics.[20] With disorders, NEGF-DFT formalism needs to be generalized to NECPA-DFT formalism, which is the subject of this section.

Notice that NECPA is only applicable to systems with substitutional disorders. To apply NECPA to DFT, one has to work with localized atomic orbitals in which only onsite blocks are different between the host atom and impurity atom. There are many kinds of atomic orbital methods that have been proved to work well with CPA, for instance,

LMTO (linear muffin-tin orbital[21,22]), KKR (Korringa-Kohn-Rostoker[23,24]), FPLO (full potential localized orbital[25]), etc. It is straightforward to generalize CPA-DFT formalism of those atomic orbital methods to NECPA-DFT formalism. For a concrete example, the NECPA-LMTO method will be presented below in details.

LMTO is an atomic orbital implementation of DFT that has been widely applied for decades in material physics to investigate electronic structures of alloys, surfaces, and interfaces. For technical details of LMTO, we refer interested readers to the monographs of Refs. 4, 21, and 22. In this section, we shall follow the notation and terminology of Ref. 4, and limit the LMTO formalism to the minimum that is necessary for implementing NECPA.

Within LMTO there are two types of Green's functions: physical Green's function and auxiliary Green's function. The physical Green's function is directly related to physical quantities, while the auxiliary Green's function is the right one to apply NECPA. The relation between disorder-averaged physical Green's function ($\overline{G^r_{iq}}$ and $\overline{G^<_{iq}}$) and auxiliary Green's function ($\overline{g^r_{iq}}$ and $\overline{g^<_{iq}}$) is as follows:

$$\begin{aligned}\overline{G^r_{iq}} &= \lambda_{iq} + \mu_{iq}\overline{g^r_{iq}}\mu_{iq},\\ \overline{G^<_{iq}} &= \mu_{iq}\overline{g^<_{iq}}\mu_{iq},\end{aligned} \tag{39}$$

where

$$\begin{aligned}\lambda_{iq} &\equiv \frac{\gamma_{iq}-\alpha}{\Delta_{iq}+(\gamma_{iq}-\alpha)(E-C_{iq})},\\ \mu_{iq} &\equiv \frac{\sqrt{\Delta_{iq}}}{\Delta_{iq}+(\gamma_{iq}-\alpha)(E-C_{iq})}.\end{aligned}$$

In these expressions, E is the energy, α is the screening constant, C_{iq}, Δ_{iq}, γ_{iq} are potential parameters of site i and component q. Notice that in LMTO all the onsite variables (e.g., $\overline{g^r_{iq}}$, $\overline{g^<_{iq}}$, $\overline{G^r_{iq}}$, $\overline{G^<_{iq}}$, λ_{iq}, μ_{iq}) are $(l_{\max}+1)^2$-by-$(l_{\max}+1)^2$ matrices in which $l_{\max}$ is the maximum orbital angular momentum quantum number at the atomic site. Especially, C_{iq}, Δ_{iq}, γ_{iq}, α are diagonal matrices of size $(l_{\max}+1)^2$-by-$(l_{\max}+1)^2$. Since all the derivations of this work do not assume that onsite variables are scalars, the formulation of NECPA remains unchanged in LMTO.

To apply NECPA to auxiliary Green's functions $\overline{g^r_{iq}}$ and $\overline{g^<_{iq}}$, one simply needs to carry out the following replacement in Eqs. (31) and (32):

$$\begin{aligned}G &\longrightarrow g,\\ H^0_C(k) &\longrightarrow S(k),\\ E-\varepsilon_{iq} &\longrightarrow P_{iq}(E),\\ E-\tilde{\varepsilon}^r &\longrightarrow \tilde{P}^r(E),\\ -\tilde{\varepsilon}^< &\longrightarrow \tilde{P}^<(E).\end{aligned} \tag{40}$$

The left-hand side is the variable in general formulation and the right-hand side is the variable in LMTO language: g is the auxiliary Green's function; $S(k)$ is the Fourier transform of structure constant; $P_{iq}(E)$ is the potential function defined as

$$P_{iq}(E) \equiv \frac{E-C_{iq}}{\Delta_{iq}+\left(\gamma_{iq}-\alpha\right)\left(E-C_{iq}\right)};$$

$\tilde{P}^r$ and $\tilde{P}^<$ are retarded and lesser coherent potentials

$$\begin{aligned}\tilde{P}^r &\equiv \mathrm{diag}\left(\left[\tilde{P}^r_1,\tilde{P}^r_2,\ldots\right]\right),\\ \tilde{P}^< &\equiv \mathrm{diag}\left(\left[\tilde{P}^<_1,\tilde{P}^<_2,\ldots\right]\right).\end{aligned}$$

Once $\overline{g^r_{iq}}$ and $\overline{g^<_{iq}}$ are solved from the NECPA equations, $\overline{G^r_{iq}}$ and $\overline{G^<_{iq}}$ can be calculated with Eq. (39). Consequently, physical quantities can be evaluated with these averaged Green's functions. The occupation number of site i and species q is obtained following Eq. (6):

$$N_{iq} = \mathrm{Im}\int \frac{dE}{2\pi}\mathrm{Tr}\,\overline{G^<_{iq}}. \tag{41}$$

The density of states (DOS) is obtained by statistically weighted contributions of DOS from each species q:

$$D = -\frac{1}{\pi}\mathrm{Im}\,\mathrm{Tr}\sum_{iq} x_{iq}\overline{G^r_{iq}}. \tag{42}$$

The transmission coefficient is obtained following Eq. (13):

$$T = \int_{-\pi}^{+\pi}\frac{dk}{2\pi}\mathrm{Tr}\,\overline{g^<_L}(k)\,\Gamma_R(k), \tag{43}$$

in which $\overline{g^<_L}(k)$ is defined as $\overline{g^<}(k)$ with the substitution $f_L \to -i$ and $f_R \to 0$.

So far, given potential parameters C_{iq}, Δ_{iq}, γ_{iq}, disorder-averaged Green's functions and physical quantities can be obtained by solving the NECPA equation. The complexity of the NECPA-LMTO method comes from the fact that potential parameters in turn depend on physical quantities and are unknown *a priori*. Therefore, potential parameters must be solved self-consistently together with disorder-averaged Green's functions. The flowchart for the self-consistent procedure of the NECPA-LMTO method is plotted in Appendix F.

As an implementation of the NECPA-LMTO method, recently a new simulation tool NANODSIM has been developed.[26] The software aims at simulating nonequilibrium quantum transport properties of realistic nanoelectronic devices from atomistic first principles. Some rather unique features are worth mentioning, including (i) it solves device Hamiltonian of two-probe systems with atomic disorders at nonequilibrium self-consistently within the general formalism of NECPA-DFT; (ii) it is capable to simulate devices containing a few thousand atomic sites on a moderate computer cluster;[27] (iii) it has implemented a recently proposed semilocal exchange-correlation potential[28] thus providing good predictions of band gaps and dispersions for many common semiconductors;[29] (iv) it has implemented a new post-analysis tool, transmission fluctuation analyzer, to predict device variability due to random discrete dopants.[30]

NANODSIM has been applied successfully to investigate nanoscaled devices. In Ref. 31, the electronic potentials are simulated atomically for Si nanotransistor channels with both n and p doping. The results are in essentially perfect agreement with those obtained by industrial TCAD software based on multitudes of material and electronic input parameters. In Ref. 32, realistic and important device physics problems have been investigated providing useful microscopic insights to improve device performance, namely, how controlled localized doping distributions in nanoscale Si transistors can suppress

leakage currents. In Ref. 33, the band offset of the GaAs/$Al_xGa_{1-x}As$ heterojunctions is investigated for the entire range of the Al doping concentration $0 < x \leqslant 1$. The calculated band structures of the GaAs and AlAs crystals and band gaps of the $Al_xGa_{1-x}As$ alloys are in very good agreement with the experimental results. We refer interested readers to this literature for further details of NANODSIM simulations of disorder effects in device physics.

VII. SUMMARY

In this work, we report the theory of NECPA for analyzing disorder effects in nonequilibrium quantum transport. Disorder average is done within CPA on the complex-time contour, which provides a *unified derivation* of $\overline{G^r}$ and $\overline{G^<}$. To accomplish the analytic continuation, the celebrated Langreth theorem is generalized to include inverse operation. By applying the generalized Langreth theorem to the contour-ordered CPA equation, the NECPA equations [Eqs. (24) and (25)] are derived for $\overline{G^r}$ and $\overline{G^<}$. In the low-concentration limit, a set of analytical solutions [Eqs. (26) and (27)] have been obtained for NECPA equations. For two-probe systems with transverse periodicity, NECPA equations need to be adapted to include k sampling in the transverse dimensions, as derived in Eqs. (31) and (32).

Although the NECPA theory is mathematically equivalent to the CPA-NVC theory developed previously, it has several advantages: (i) NECPA is elegant from a theoretical point of view due to its simplicity and unification; (ii) the conditional Green's functions $\overline{G^r_{iq}}$ and $\overline{G^<_{iq}}$ are derived for disorder sites beyond the binary situation; (iii) stable iterative solution methods are available for solving NECPA equations.

The accuracy of the NECPA equation has been numerically verified by comparing to brute force calculations of TB models. It is also demonstrated that NECPA can be combined with the DFT technique to enable atomistic first-principles simulation of quantum transport. A simulation tool, NANODSIM, has been developed as an implementation of NECPA-LMTO method. The software has already been applied to a number of important and interesting device physics problems.

Finally, we would like to mention that NECPA equations are not limited to combine with DFT. It is straightforward to apply NECPA to other atomistic device models such as tight-binding models. In addition, the generalized Langreth theorem [Eqs. (18)–(23)] can be applied to other NEGF techniques (e.g, equation of motion) so that G^r and $G^<$ are derived in a unified and consistent way.

ACKNOWLEDGMENTS

We thank Y. Ke for many discussions concerning the CPA-NVC theory and its LMTO implementation. We thank K. Xia for useful discussions on the LMTO method of DFT. We thank Y. Hu for many discussions on computational issues of the NECPA-LMTO and the NANODSIM software. We thank J. Maassen, F. Zahid, Y. Wang, and P. Zhang for many discussions on practical applications of the NECPA-LMTO and the NANODSIM software for first-principles quantum transport simulations. The financial support from NRC-IRAP of Canada is gratefully acknowledged.

APPENDIX A: DERIVATION OF EQS. (16) AND (17)

In this appendix, we derive Eqs. (16) and (17)) by using contour-ordered CPA equation ((15) and the definition of the conditional Green's function. First, we prove a lemma for the block matrix inverse. Assume that A and A' are the inverse of following block matrices which are composed of 2×2 matrix blocks:

$$A = \begin{pmatrix} a_{11} & a_{12} \\ a_{21} & a_{22} \end{pmatrix}^{-1},$$
$$A' = \begin{pmatrix} a'_{11} & a_{12} \\ a_{21} & a_{22} \end{pmatrix}^{-1}.$$

It is straightforward to obtain

$$A_{11} = \left(a_{11} - a_{12}a_{22}^{-1}a_{21}\right)^{-1},$$
$$A'_{11} = \left(a'_{11} - a_{12}a_{22}^{-1}a_{21}\right)^{-1}.$$

It follows

$$(A_{11})^{-1} - (A'_{11})^{-1} = a_{11} - a'_{11}, \tag{A1}$$

which is the conclusion of the lemma.

Second, we apply the lemma to $\overline{G_i}$ and $\overline{G_{iq}}$ and obtain a useful relation between them. $\overline{G_i}$ and $\overline{G_{iq}}$ are defined in the second and third lines of Eq. (16). Let $A = \overline{G_i}$ and $A' = \overline{G_{iq}}$, and reorder $\overline{G_i}$ and $\overline{G_{iq}}$ such that the block of site i is in the location of a_{11} and a'_{11}, respectively. Due to the definition of $\tilde{\varepsilon}$ and $\tilde{\varepsilon}^{iq}$,

$$a_{11} - a'_{11} = (-\tilde{\varepsilon})_{ii} - (-\tilde{\varepsilon}^{iq})_{ii} = (-\tilde{\varepsilon}_i) - (-\varepsilon_{iq}).$$

By using the lemma, it is derived

$$(\overline{G_i})^{-1} - (\overline{G_{iq}})^{-1} = \varepsilon_{iq} - \tilde{\varepsilon}_i. \tag{A2}$$

Third, we derive the first line of Eq. (16). Substitute Eq. (A2) into the second line of Eq. (15) and obtain

$$t_{iq} = \{[(\overline{G_i})^{-1} - (\overline{G_{iq}})^{-1}]^{-1} - \overline{G_i}\}^{-1}. \tag{A3}$$

Substitute Eq. (A3) into the first line of Eq. (15) and obtain

$$\sum_q x_{iq}\{[(\overline{G_i})^{-1} - (\overline{G_{iq}})^{-1}]^{-1} - \overline{G_i}\}^{-1} = 0.$$

By using $\sum_q x_{iq} = 1$, Eq. (A3) can be simplified as

$$\sum_q x_{iq}\overline{G_{iq}} = \overline{G_i}, \tag{A4}$$

which is the first line of Eq. (16).

Finally, we derive the fourth and fifth lines of Eq. (17) from Eq. (16). As shown above, Eq. (16) leads to Eq. (A2), due to which one can always find a proper Ω_i such that

$$(\overline{G_i})^{-1} = E - \tilde{\varepsilon}_i - \Omega_i, \tag{A5}$$

$$(\overline{G_{iq}})^{-1} = E - \varepsilon_{iq} - \Omega_i, \tag{A6}$$

which are equivalent to the fourth and fifth lines of Eq. (17).

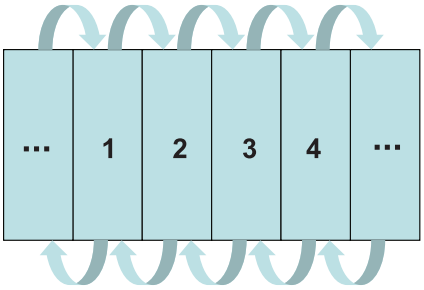

FIG. 5. (Color online) Schematic plot showing the partition of a two-probe system into principal layers along the transport direction. The integers label the PLs. Partition is done in such a way that each PL only couples to its nearest-neighbor PLs.

APPENDIX B: NECPA WITH PRINCIPAL-LAYER ALGORITHM

In most two-probe systems, the size along the transport dimension is much larger than their transverse dimensions. A two-probe system can therefore be partitioned into principal layers (PL) along the transport direction such that each PL only interacts with its two nearest-neighbor PLs, as shown in Fig. 5. Once a two-probe system is partitioned into PLs, the calculation of $\overline{G^r}$ and $\overline{G^<}$ can be reduced to $\overline{G^r} = H^{-1}$ and $\overline{G^<} \equiv \frac{1}{i} H^{-1} D (H^\dagger)^{-1}$. Here, $H \equiv E - H_C^0 - \tilde{\varepsilon}^r - \Sigma^r$ is a block-tridiagonal matrix which has the following nonzero pattern (illustrated with $N = 4$ PLs):

$$H = \begin{array}{|c|c|c|c|} \hline H_{11} & H_{12} & O & O \\ \hline H_{21} & H_{22} & H_{23} & O \\ \hline O & H_{32} & H_{33} & H_{34} \\ \hline O & O & H_{43} & H_{44} \\ \hline \end{array}, \tag{B1}$$

where H_{ij} are nonzero blocks, O the zero blocks, and subscripts i, j label the PLs. $D \equiv i\,(\Sigma^< + \tilde{\varepsilon}^<)$ is a Hermitian block-diagonal matrix which has the following nonzero pattern (illustrated with $N = 4$ PLs):

$$D = \begin{array}{|c|c|c|c|} \hline D_1 & O & O & O \\ \hline O & D_2 & O & O \\ \hline O & O & D_3 & O \\ \hline O & O & O & D_4 \\ \hline \end{array}, \tag{B2}$$

where $D_i = D_i^\dagger$ and subscript i labels the PLs.

The calculation of $\overline{G^r}$ and $\overline{G^<}$ in the NECPA equations involves matrix inversion and multiplication of these sparse matrices. The computational cost of full matrix inversion and multiplication is of $O(N^3)$ which becomes the bottleneck for large N. Fortunately, only the diagonal elements of the Green's functions are needed in solving NECPA equations. By taking the advantage of the zero blocks in Eqs. (B1) and (B2), the cost of calculating the diagonal elements can be reduced to $O\,(N)$.[34,35]

Following Ref. 34, the calculation of diagonal elements of $\overline{G^r}$ can be accomplished with the following recursive relation:

$$\begin{aligned} \overline{G^r_{ii}} &\equiv A_i, \quad C_1 = H_{11}^{-1}, \\ C_{i+1} &= (H_{i+1,i+1} - H_{i+1,i} C_i H_{i,i+1})^{-1}, \quad A_N = C_N, \\ A_i &= C_i + C_i H_{i,i+1} A_{i+1} H_{i+1,i} C_i . \end{aligned}$$

Following Ref. 35, the calculation of diagonal blocks of $\overline{G^<}$ can be accomplished with the following recursive relation:

$$\begin{aligned} \overline{G^<_{ii}} &\equiv \frac{1}{i} B_i, \\ Y_1 &= D_1, \\ Y_i &= D_i + H_{i,i-1} C_{i-1} Y_{i-1} C_{i-1}^\dagger H_{i,i-1}^\dagger, \\ B_N &= C_N Y_N C_N^\dagger, \\ B_i &= C_i H_{i,i+1} B_{i+1} H_{i,i+1}^\dagger C_i^\dagger - C_i Y_i C_i^\dagger \\ &\quad + A_i Y_i C_i^\dagger + (A_i Y_i C_i^\dagger)^\dagger . \end{aligned}$$

The principal-layer algorithm helps to optimize the performance of iterative methods for solving NECPA equations.

APPENDIX C: NECPA AND CPA-NVC: THE EQUIVALENCE

In this appendix, we prove that $\overline{G^<}$ solved from NVC equations (33) and (34) are identical to $\overline{G^<}$ solved from NECPA equation (25) under the condition of NECPA equation (24) for $\overline{G^r}$. Since the only difference between the expressions of $\overline{G^<}$ in NECPA equation (25) and NVC equation (33) are $\tilde{\varepsilon}^<$ and Λ, we proceed to prove that these two quantities are actually identical. The NVC equation for Λ [Eq. (34)] is a nonhomogeneous linear equation which has a unique solution. Hence, the equivalence is proved if $\tilde{\varepsilon}^<$ satisfies Eq. (34). It is shown in the following that $\tilde{\varepsilon}^<$ obtained from NECPA equation (25) indeed satisfies Eq. (34).

We start by eliminating $\Omega_i^<$ from Eq. (25):

$$\begin{aligned} \overline{G_i^<} &= \sum_q x_{iq} \overline{G_{iq}^<} = \sum_q x_{iq} \overline{G_{iq}^r} \Omega_i^< \overline{G_{iq}^a} \\ &= \sum_q x_{iq} \overline{G_{iq}^r} \left[\left(\overline{G_i^r}\right)^{-1} \overline{G_i^<} \left(\overline{G_i^a}\right)^{-1} - \tilde{\varepsilon}_i^< \right] \overline{G_{iq}^a}. \end{aligned} \tag{C1}$$

Next, we eliminate quantities E, ε_{iq}, and $\tilde{\varepsilon}_i^r$ from the expressions of $\overline{G_{iq}^r}$, $\overline{G_i^r}$, and t_{iq}^r [see Eqs. (24) and (14)]:

$$\begin{aligned} \overline{G_{iq}^r} &= \left[E - \varepsilon_{iq} - \Omega_i^r \right]^{-1}, \\ \overline{G_i^r} &= \left[E - \tilde{\varepsilon}_i^r - \Omega_i^r \right]^{-1}, \\ t_{iq}^r &\equiv \left[\left(\varepsilon_{iq} - \tilde{\varepsilon}_i^r \right)^{-1} - \overline{G_i^r} \right]^{-1}, \end{aligned}$$

and obtain

$$\overline{G_{iq}^r} = \overline{G_i^r} \left(1 + t_{iq}^r \overline{G_i^r} \right). \tag{C2}$$

Finally, inserting Eq. (C2) into (C1) and using the CPA condition of the first line of Eq. (14),

$$\sum_q x_{iq} t_{iq}^r = \sum_q x_{iq} t_{iq}^a = 0,$$

we derive an equation for the quantity $\tilde{\varepsilon}_i^<$:

$$\begin{aligned} \tilde{\varepsilon}_i^< &= \sum_q x_{iq} t_{iq}^r \overline{G_i^<} t_{iq}^a - \sum_q x_{iq} t_{iq}^r \overline{G_i^r} \tilde{\varepsilon}_i^< \overline{G_i^a} t_{iq}^a \\ &= \sum_q x_{iq} t_{iq}^r [\overline{G^r} \left(\Sigma^< + \tilde{\varepsilon}^< \right) \overline{G^a}]_{ii} t_{iq}^a \\ &\quad - \sum_q x_{iq} t_{iq}^r \overline{G_i^r} \tilde{\varepsilon}_i^< \overline{G_i^a} t_{iq}^a, \end{aligned} \tag{C3}$$

which is identical to Eq. (34).

APPENDIX D: NECPA FOR BINARY DISORDER SYSTEM

In this appendix, we show that for binary systems $q = A, B$, the conditional Green's functions solved from NECPA equations (24) and (25) are precisely given by Eqs. (37) and (38) which are obtained from the random variable method discussed in Sec. IV C.

First, we focus on retarded conditional Green's functions $\overline{G^r_{iA}}$ and $\overline{G^r_{iB}}$. Let $\overline{G^r_{iA}} = \lambda_{iA}\overline{G^r_i}$ and $\overline{G^r_{iB}} = \lambda_{iB}\overline{G^r_i}$, and we proceed to solve for the two coefficients λ_{iA} and λ_{iB}. For the $q = A, B$ binary situation, NECPA equation (24) is reduced to the following form:

$$\begin{aligned}
\overline{G^r_i} &= x_{iA}\overline{G^r_{iA}} + x_{iB}\overline{G^r_{iB}},\\
\overline{G^r_i} &= \left(E - \tilde{\varepsilon}^r_i - \Omega^r\right)^{-1},\\
\overline{G^r_{iA}} &= \left(E - \varepsilon_{iA} - \Omega^r\right)^{-1},\\
\overline{G^r_{iB}} &= \left(E - \varepsilon_{iB} - \Omega^r\right)^{-1}.
\end{aligned}$$

By eliminating quantities $\overline{G^r_i}$, $\overline{G^r_{iA}}$, $\overline{G^r_{iB}}$, and $E - \Omega^r$ from the above, we obtain

$$\begin{aligned}
&x_{iA}\lambda_{iA} + x_{iB}\lambda_{iB} = 1,\\
&\left(\tilde{\varepsilon}^r_i - \varepsilon_{iA}\right)\left(\lambda^{-1}_{iA} - 1\right)^{-1} = \left(\tilde{\varepsilon}^r_i - \varepsilon_{iB}\right)\left(\lambda^{-1}_{iB} - 1\right)^{-1}.
\end{aligned} \tag{D1}$$

By using the normalization of probability $x_{iA} + x_{iB} = 1$, λ_{iA} and λ_{iB} can be solved after some algebra:

$$\begin{aligned}
\lambda_{iA} &= \frac{1}{x_{iA}}(\varepsilon_{iA} - \varepsilon_{iB})^{-1}\left(\tilde{\varepsilon}^r_i - \varepsilon_{iB}\right),\\
\lambda_{iB} &= \frac{1}{x_{iB}}(\varepsilon_{iB} - \varepsilon_{iA})^{-1}\left(\tilde{\varepsilon}^r_i - \varepsilon_{iA}\right),
\end{aligned}$$

which are identical to Eq. (37) obtained from the random variable method.

Similarly, the lesser conditional Green's functions $\overline{G^<_{iA}}$ and $\overline{G^<_{iB}}$ can be solved from NECPA equation (25) and proved to be identical to Eq. (38) which is obtained from the random variable method. However, the algebra turns out to be extremely tedious. An alternative way is to play the same trick as in the derivation of NECPA equations, namely, we generalize Eq. (37) to a contour-ordered form by simply removing the superscript r:

$$\begin{aligned}
\overline{G_{iA}} &= \frac{1}{x_{iA}}(\varepsilon_{iA} - \varepsilon_{iB})^{-1}(\tilde{\varepsilon}_i - \varepsilon_{iB})\,\overline{G_i},\\
\overline{G_{iB}} &= \frac{1}{x_{iB}}(\varepsilon_{iB} - \varepsilon_{iA})^{-1}(\tilde{\varepsilon}_i - \varepsilon_{iA})\,\overline{G_i}.
\end{aligned}$$

Now, we apply the generalized Langreth theorem to these two equations and straightforwardly obtain Eq. (38).

APPENDIX E: NECPA EQUATIONS FOR THE TB MODELS

In the appendix, we list the NECPA equations as applied to the TB models. For the 1D TB model, NECPA equations (24) and (25) are reduced to the following form:

$$\begin{aligned}
\overline{G^r_i} &= \sum_q x_{iq}G^r_{iq},\\
\overline{G^r} &= \left[E - \begin{pmatrix}\tilde{\varepsilon}^r_1 & t\\ t & \tilde{\varepsilon}^r_2\end{pmatrix} - \begin{pmatrix}\Sigma^r_0 & 0\\ 0 & \Sigma^r_0\end{pmatrix}\right]^{-1},\\
\overline{G^r_i} &= [\overline{G^r}]_{ii},\\
\overline{G^r_i} &= \left(E - \tilde{\varepsilon}^r_i - \Omega^r_i\right)^{-1},\\
G^r_{iq} &= \left(E - \varepsilon_{iq} - \Omega^r_i\right)^{-1}.
\end{aligned} \tag{E1}$$

$$\begin{aligned}
\overline{G^<_i} &= \sum_q x_{iq}G^<_{iq},\\
\overline{G^<} &= \overline{G^r}\left[\begin{pmatrix}\tilde{\varepsilon}^<_1 & 0\\ 0 & \tilde{\varepsilon}^<_2\end{pmatrix} + \begin{pmatrix}if_L\Gamma_0 & 0\\ 0 & if_R\Gamma_0\end{pmatrix}\right]\overline{G^a},\\
\overline{G^<_i} &= [\overline{G^<}]_{ii},\\
\overline{G^<_i} &= \overline{G^r_i}(\tilde{\varepsilon}^<_i + \Omega^<_i)\overline{G^a_i},\\
G^<_{iq} &= G^r_{iq}\Omega^<_i G^a_{iq},
\end{aligned} \tag{E2}$$

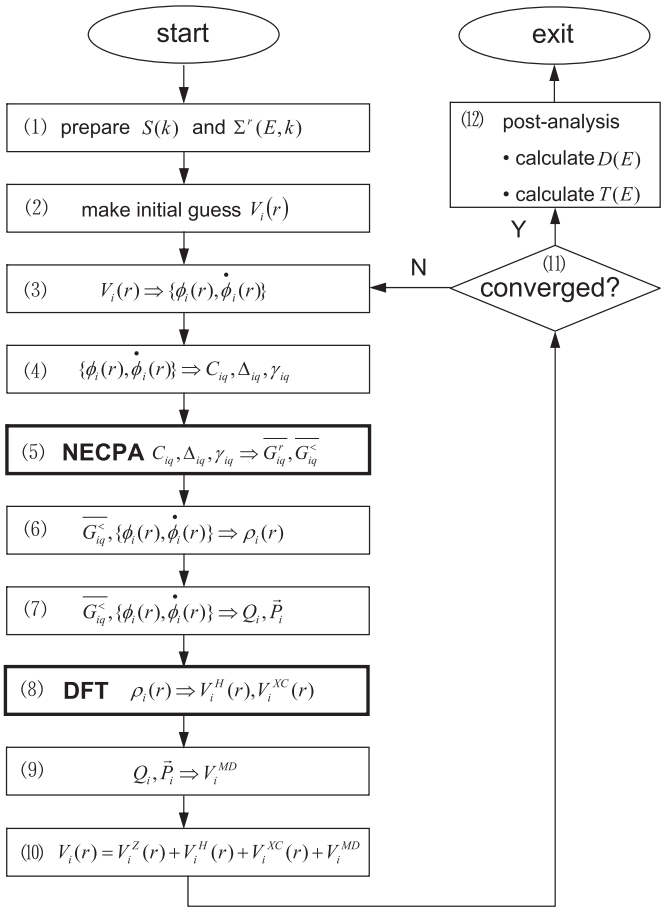

FIG. 6. Flowchart of the NECPA-LMTO self-consistent procedure that is implemented in the NANODSIM quantum transport package. For clarity, the steps of NECPA and DFT have been highlighted.

in which Γ_0 and Σ_0^r have been defined in Sec. V A. Equations (E1) and (E2) are used in the NECPA calculation of the 1D TB model presented in Sec. V A.

The 2D two-probe model in Sec. V B has transverse periodicity, hence NECPA equations (31) and (32) are applied. For the 2D TB model, they are reduced to the following form:

$$\begin{aligned}
\overline{G^r} &= \sum_q x_q G_q^r, \\
\overline{G^r} &= \int_{-\pi}^{+\pi} \frac{dk}{2\pi} \left[E - 2t\cos k - \tilde{\varepsilon}^r - 2\Sigma_0^r(k)\right]^{-1}, \\
\overline{G^r} &= (E - \tilde{\varepsilon}^r - \Omega^r)^{-1}, \\
G_q^r &= (E - \varepsilon_q - \Omega^r)^{-1}.
\end{aligned} \tag{E3}$$

$$\begin{aligned}
\overline{G^<} &= \sum_q x_q G_q^<, \\
\overline{G^<} &= \int_{-\pi}^{+\pi} \frac{dk}{2\pi} \frac{i f_L \Gamma_0(k) + i f_R \Gamma_0(k)}{\left|E - 2t\cos k - \tilde{\varepsilon}^r - 2\Sigma_0^r(k)\right|^2}, \\
\overline{G^<} &= \overline{G^r}\left(\tilde{\varepsilon}^< + \Omega^<\right)\overline{G^a}, \\
G_q^< &= G_q^r \Omega^< G_q^a,
\end{aligned} \tag{E4}$$

in which $\Gamma_0(k) = -2\,\mathrm{Im}\Sigma_0^r(k)$ and $\Sigma_0^r(k)$ is the Fourier transform of the electrode self-energy:

$$\Sigma_0^r(k) = \xi\left(\frac{E + i0^+ - \varepsilon_0 - 2t\cos k}{t}\right)t.$$

The expression of $\xi(z)$ can be found in Sec. V A. Equations (E3) and (E4) are used in the NECPA calculation of the 2D TB model presented in Sec. V B.

APPENDIX F: FLOWCHART OF NECPA-LMTO METHOD

The flowchart for the self-consistent procedure of NECPA-LMTO method is sketched in Fig. 6 and explained as follows.

(1) Prepare the structure constant $S(k)$ and the lead self-energies $\Sigma_\beta^r(E,k)$.

(2) Make an initial guess of the atomic potential $V_i(r)$ for site i.

(3) Calculate orbitals $\{\phi_i(r),\dot{\phi}_i(r)\}$ by solving Schrödinger equation in the potential $V_i(r)$.

(4) Calculate potential parameters C_{iq}, Δ_{iq}, γ_{iq} with Wronskians involving $\phi_i(r)$ and $\dot{\phi}_i(r)$.

(5) NECPA: Obtain disorder-averaged Green's functions $\overline{G_{iq}^r}$, $\overline{G_{iq}^<}$ by solving NECPA equation containing C_{iq}, Δ_{iq}, γ_{iq} [see Eqs. (39), (31), (32), and (40)].

(6) Calculate the atomic charge density $\rho_i(r)$ by using $\overline{G_{iq}^<}$ and $\{\phi_i(r),\dot{\phi}_i(r)\}$.

(7) Calculate the monopole Q_i and the dipole $\overrightarrow{P_i}$ by using $\overline{G_{iq}^<}$ and $\{\phi_i(r),\dot{\phi}_i(r)\}$.

(8) DFT: Calculate the Hartree potential $V_i^H(r)$ and the exchange-correlation potential $V_i^{\mathrm{XC}}(r)$ by using $\rho_i(r)$.

(9) Calculate the Madelung potential V_i^{MD} by using $\{Q_i, \overrightarrow{P_i}\}$ with Ewald summation.

(10) Update the atomic potential $V_i(r) = V_i^Z(r) + V_i^H(r) + V_i^{\mathrm{XC}}(r) + V_i^{\mathrm{MD}}$ where $V_i^Z(r) \equiv -\frac{Z}{r}$ is the nuclear potential.

(11) Check the convergence of $V_i(r)$. Go back to step 3 until $V_i(r)$ is fully converged for every atomic site.

(12) Carry out post analysis: calculate density of states by using Eq. (42); calculate transmission coefficient by using Eq. (43), etc.

The above procedure involves technical details of the LMTO method; we refer the interested reader to Ref. 4.

*eric@nanoacademic.ca

[1] H. Haug and A.-P. Jauho, *Quantum Kinetics in Transport and Optics of Semiconductor* (Springer, Berlin, 1996).

[2] S. Datta, *Electronic Transport in Mesoscopic System* (Cambridge University Press, Cambridge, England, 1995).

[3] P. Soven, Phys. Rev. **156**, 809 (1967); D. W. Taylor, *ibid.* **156**, 1017 (1967).

[4] I. Turek, V. Drchal, J. Kudrnovský, M. Šob, and P. Weinberger, *Electronic Structure of Disordered Alloys, Surfaces and Interfaces* (Kluwer Academic, Dordrecht, 1997).

[5] B. Velický, Phys. Rev. **184**, 614 (1969).

[6] K. Carva, I. Turek, J. Kudrnovský, and O. Bengone, Phys. Rev. B **73**, 144421 (2006).

[7] Y. Ke, K. Xia, and H. Guo, Phys. Rev. Lett. **100**, 166805 (2008), and associated Supplemental Material (E-PRLTAO-100-020817). See also Y. Q. Ke, Ph.D. thesis, McGill University, 2010.

[8] Y. Ke, K. Xia, and H. Guo, Phys. Rev. Lett. **105**, 236801 (2010).

[9] F. Zahid, Y. Ke, D. Gall, and H. Guo, Phys. Rev. B **81**, 045406 (2010).

[10] Z. Wang, Y. Ke, D. Liu, H. Guo, and K. H. Bevan, Appl. Phys. Lett. **101**, 093102 (2012).

[11] Some preliminary results were presented in the International Conference and Hands-on Workshop on Quantum Transport Theory and Nanoelectronics Simulation, August, 2011, Beijing, China: http://physics.ruc.edu.cn/workshop/2011/index.html.

[12] D. C. Langreth, in *Linear and Nonlinear Electron Transport in Solids*, edited by J. T. Devreese and V. E. Van Doren (Plenum, New York, 1976).

[13] A. P. Jauho, N. S. Wingreen, and Y. Meir, Phys. Rev. B **50**, 5528 (1994).

[14] For an atomic disorder site discussed in Sec. VI, the onsite energy is a matrix block rather than a scalar.

[15] If disorder sites appear everywhere in the electrodes which extend to $z = \pm\infty$, traveling waves will not be able to propagate and no current can flow.

[16] L. P. Kadanoff and G. Baym, *Quantum Statistical Mechanics* (Benjamin, New York, 1962).

[17] In the literature, coherent interactor actually refers to retarded coherent interactor; see, e.g., J. Kudrnovský and V. Drchal, Phys. Rev. B **41**, 7515 (1990).

[18] From the Feynman diagrammatic point of view, both CPA and NVC neglect diagrams with crossing impurity lines and discard diagrams with dangling impurity lines. Since the diagram structures of CPA and NVC are different, it is not immediately transparent why the neglected terms are equal.

[19]To derive $\overline{G^r_{iq}}$, see Eqs. (4.21) and (4.22) in Ref. 4. To derive $\overline{G^<_{iq}}$, see Eqs. (28) and (29) in the Supplemental Material of Ref. 7 (E-PRLTAO-100-020817).

[20]J. Taylor, H. Guo, and J. Wang, Phys. Rev. B **63**, 121104(R) (2001).

[21]O. K. Andersen, O. Jepsen, and D. Glötzel, in *Highlights of Condensed-Matter Theory*, edited by F. Bassani, F. Fumi, and M. P. Tosi (North-Holland, New York, 1985), p. 59.

[22]H. L. Skriver, *The LMTO Method* (Springer, Berlin, 1984).

[23]J. Korringa, Physica (Amsterdam) **13**, 392 (1947).

[24]W. Kohn and N. Rostoker, Phys. Rev. **94**, 1111 (1954).

[25]K. Koepernik and H. Eschrig, Phys. Rev. B **59**, 1743 (1999); I. Opahle, K. Koepernik, and H. Eschrig, *ibid.* **60**, 14035 (1999).

[26]For more details of the NANODSIM software, please visit http://www.nanoacademic.com or contact the corresponding author of this paper.

[27]J. Maassen, M. Harb, V. Michaud-Rioux, Y. Zhu, and H. Guo, Proc. IEEE **101**, 518 (2013).

[28]F. Tran and P. Blaha, Phys. Rev. Lett. **102**, 226401 (2009).

[29]Y. Wang, H. Yin, R. Cao, F. Zahid, Y. Zhu, L. Liu, J. Wang, and H. Guo, Phys. Rev. B **87**, 235203 (2013).

[30]Y. Zhu, L. Liu, and H. Guo, Phys. Rev. B **88**, 085420 (2013).

[31]L. Zhang, F. Zahid, Y. Zhu, L. Liu, J. Wang, H. Guo, P. C. H. Chan, and M. Chan, IEEE Trans. Electron Devices **60**, 3527 (2013).

[32]J. Maassen and H. Guo, Phys. Rev. Lett. **109**, 266803 (2012).

[33]Y. Wang, F. Zahid, Y. Zhu, L. Liu, J. Wang, and H. Guo, Appl. Phys. Lett. **102**, 132109 (2013).

[34]D. Waldron, L. Liu, and H. Guo, Nanotechnology **18**, 424026 (2007).

[35]D. E. Petersen, S. Li, K. Stokbro, H. H. B. Sørensen, P. C. Hansen, S. Skelboe, and E. Darve, J. Comput. Phys. **228**, 5020 (2009).